Electronic Supplementary Information

One-pot synthesis of highly efficient MgO for the removal of Congo red in aqueous solution

*Zonquan Bai, Yajun Zheng, and Zhiping Zhang**

School of Chemistry and Chemical Engineering, Xi'an Shiyou University, Xi'an 710065,

China. Fax: +86 29 8838 2693; Tel: +86 29 8838 2694; E-mail: zhangzp0304@gmail.com.

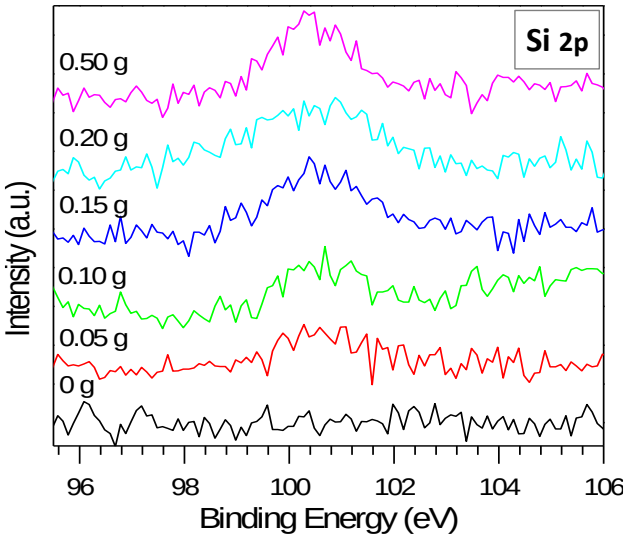

Figure S1. XPS data of the region of Si 2p for the MgO particles prepared via the reaction between $Mg(NO_3)_2$ and Na_2CO_3 in the presence of different amounts of Na_2SiO_3 (0 – 0.50 g) at 50 ºC.

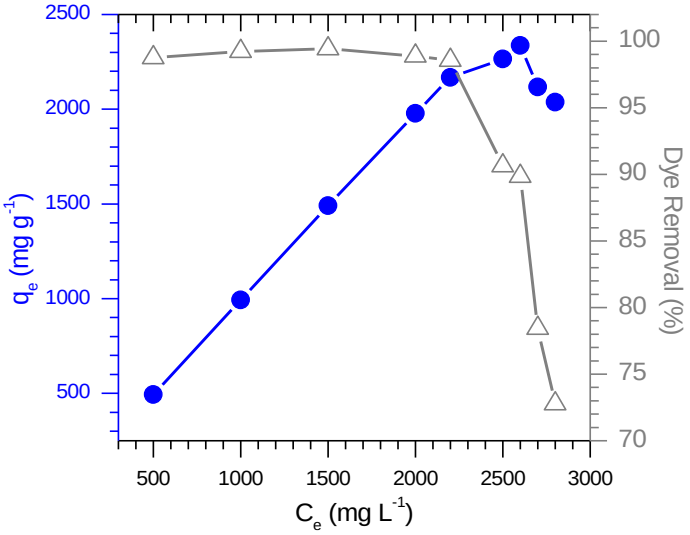

Figure S2. Adsorption isotherms of Congo red on the obtained product obtained from the system without involvement of Na_2SiO_3.

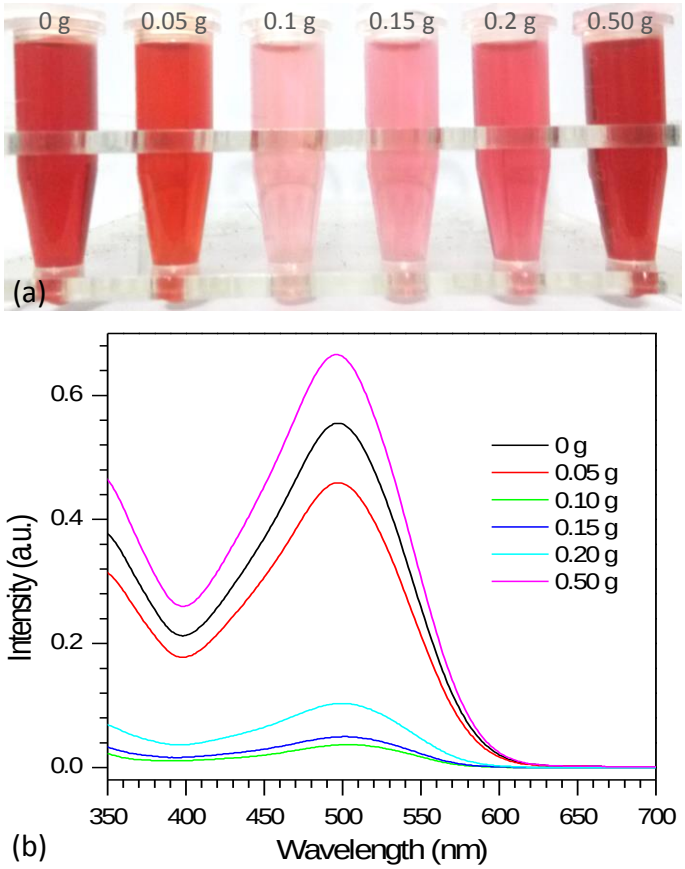

Figure S3. (a) Photograph and (b) UV-vis spectra of initial Congo red solutions (2500 mg L^{-1}, 100 mL) being treated with 100 mg of MgO particles obtained from the reaction between $Mg(NO_3)_2$ and Na_2CO_3 in the presence of various amounts of Na_2SiO_3 (0 – 0.50 g) as indicated in the figures.

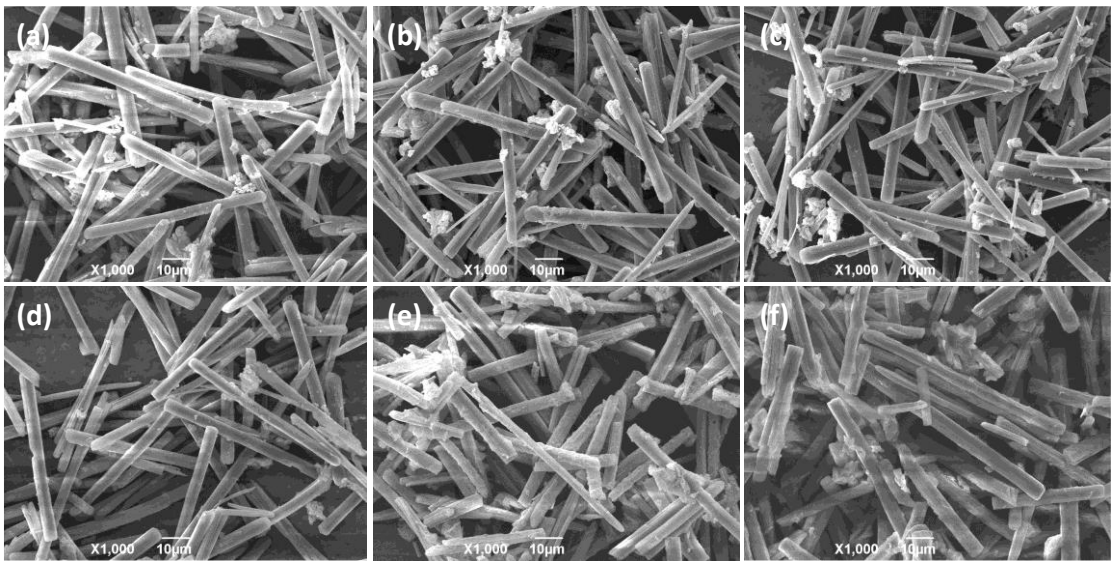

Figure S4. Typical SEM images of the obtained MgO particles by reaction of $Mg(NO_3)_2$ and Na_2CO_3 in the presence of different amounts of Na_2SiO_3: (a) 0 g; (b) 0.05 g; (c) 0.10 g; (d) 0.15 g; (e) 0.20 g; (f) 0.50 g.

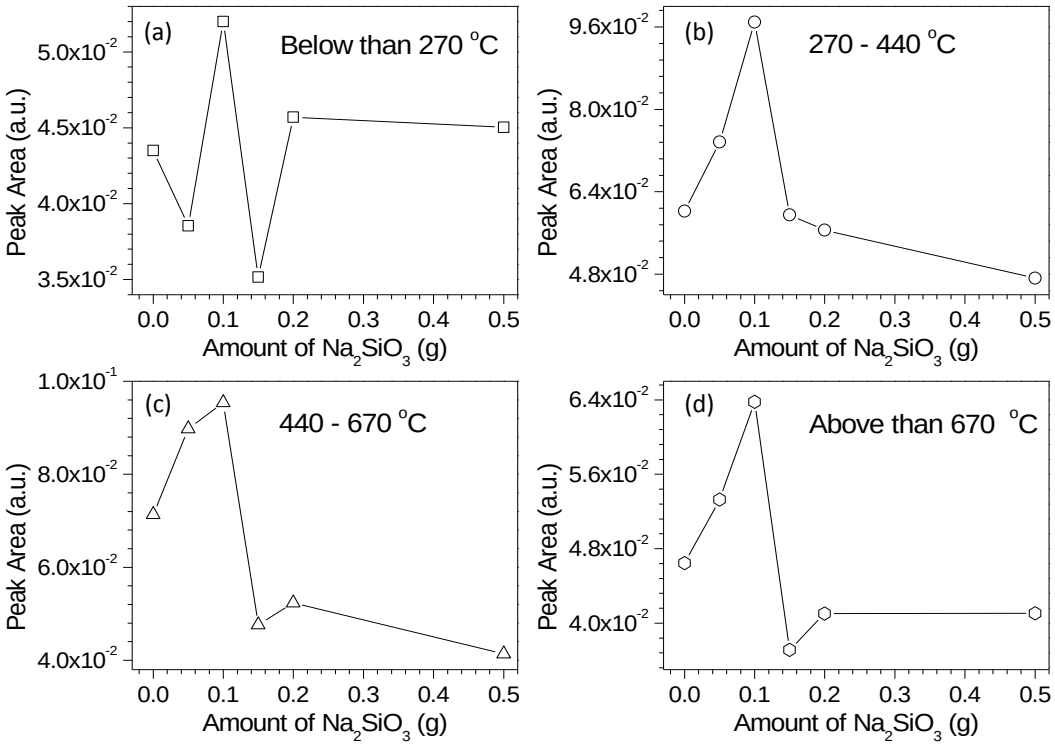

Figure S5. Correlation between the peak area of CO_2 desorption at different temperature ranges, including (a) below 270 °C, (b) 270 - 440 °C, (c) 440 - 670 °C and (d) above 670 °C, and the added amount of Na_2SiO_3 in MgO preparation.

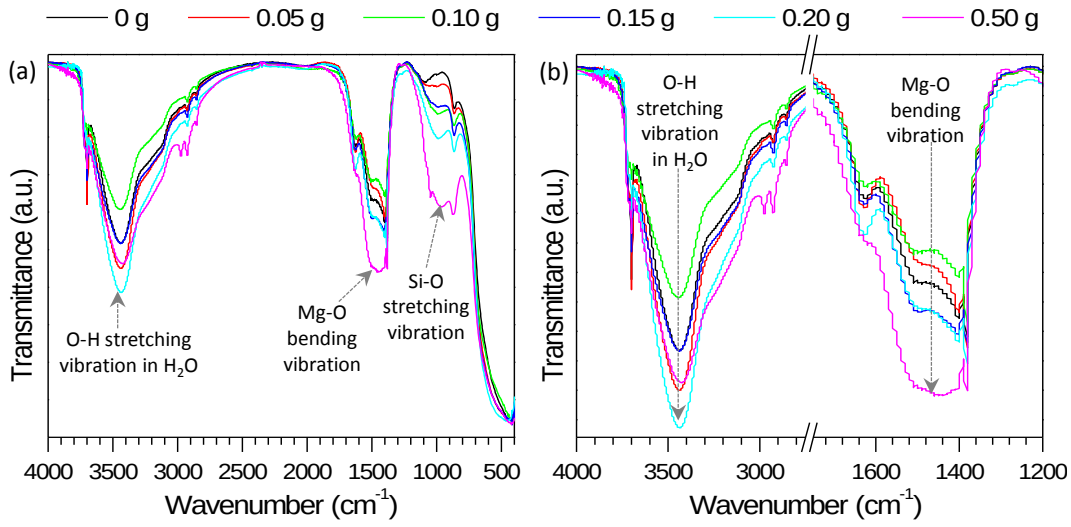

Figure S6. (a) FT-IR spectra of the obtained MgO with varying the added amount of Na_2SiO_3 in preparation and (b) their magnified wavenumber range (4000 - 1200 cm^{-1}).

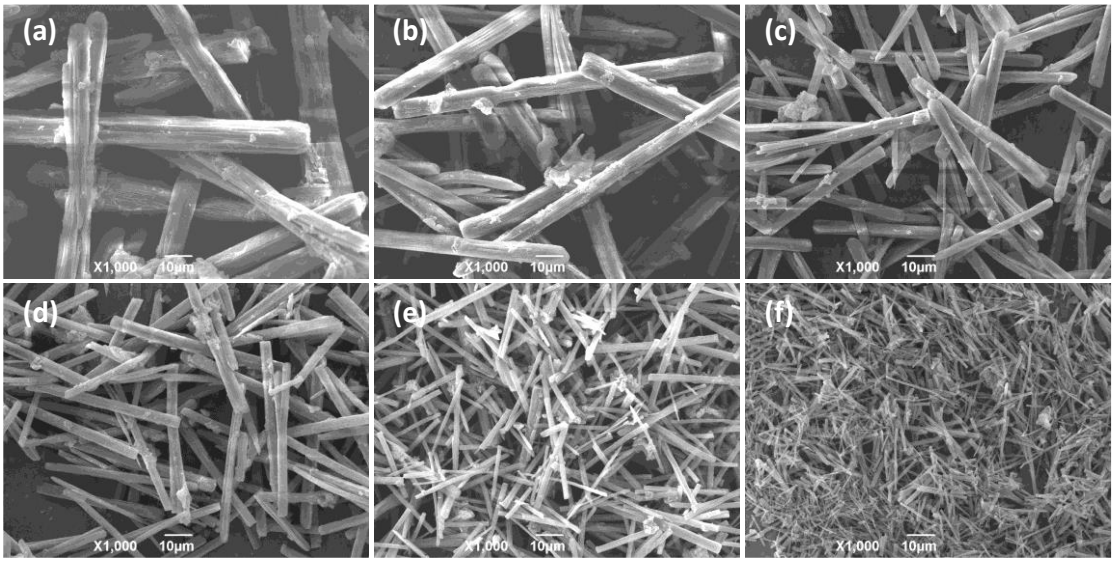

Figure S7. Typical SEM images of the obtained MgO particles by reaction of $Mg(NO_3)_2$ and Na_2CO_3 in the presence of 0.1 g Na_2SiO_3 under different stirring times with a stirring speed of around 800 rpm followed by a period of 1 h aging: (a) 0.5 min; (b) 1.0 min; (c) 1.5 min; (d) 2.0 min; (e) 2.5 min; (f) 5.0 min.

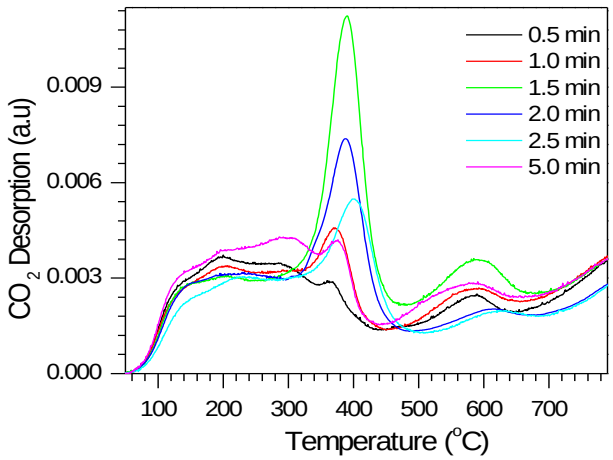

Figure S8. CO_2-TPD profiles of the MgO particles obtained from different stirring times (0.5 – 5.0 min) in the reaction system between $Mg(NO_3)_2$ and Na_2CO_3 with presence of 0.1 g Na_2SiO_3.

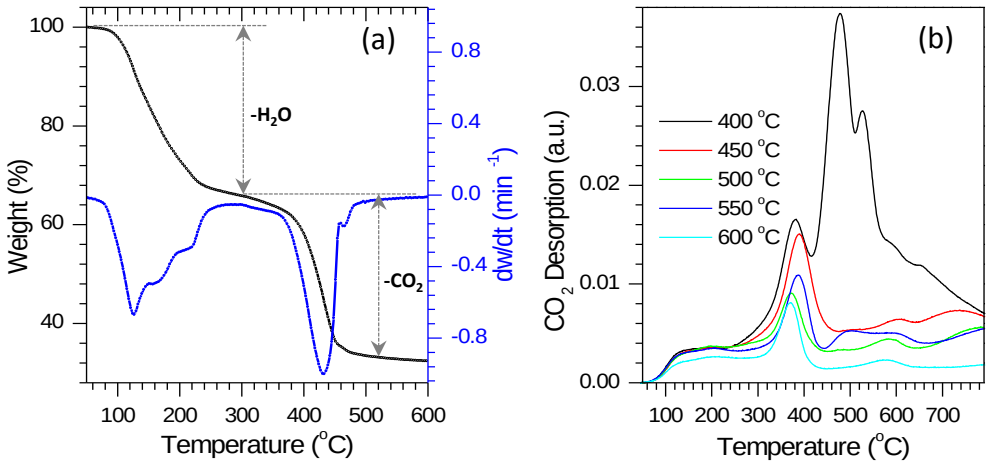

Figure S9. (a) TG-DTG curves of the obtained product by reaction of $Mg(NO_3)_2$ and Na_2CO_3 in the presence of 0.1 g Na_2SiO_3 followed by a period of 1 h aging; (b) CO_2-TPD profiles of the MgO particles obtained by calcination of their precursors at different temperatures ranging from 400 to 600 °C.

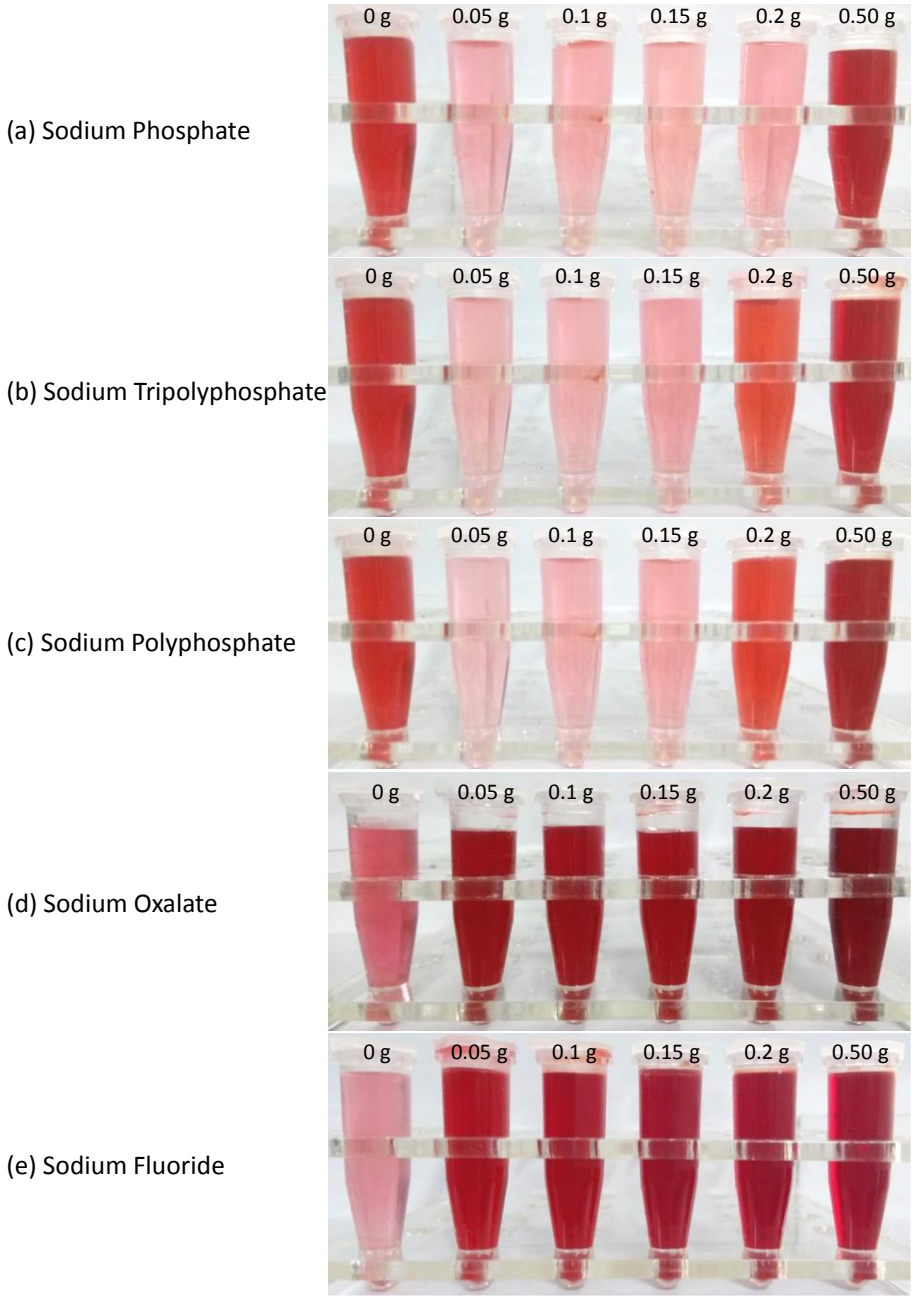

Figure S10. Photographs of the initial Congo red solutions (2500 mg L^{-1} for sodium phosphate, sodium tripolyphosphate, sodium polyphosphate, 2300 mg L^{-1} for sodium oxalate and sodium fluoride) being treated with the MgO particles obtained from the reaction between $Mg(NO_3)_2$ and Na_2CO_3 in the presence of various amounts (0 – 0.50 g) of (a) sodium phosphate; (b) sodium tripolyphosphate; (c) sodium polyphosphate; (d) sodium oxalate; and (e) sodium fluoride.

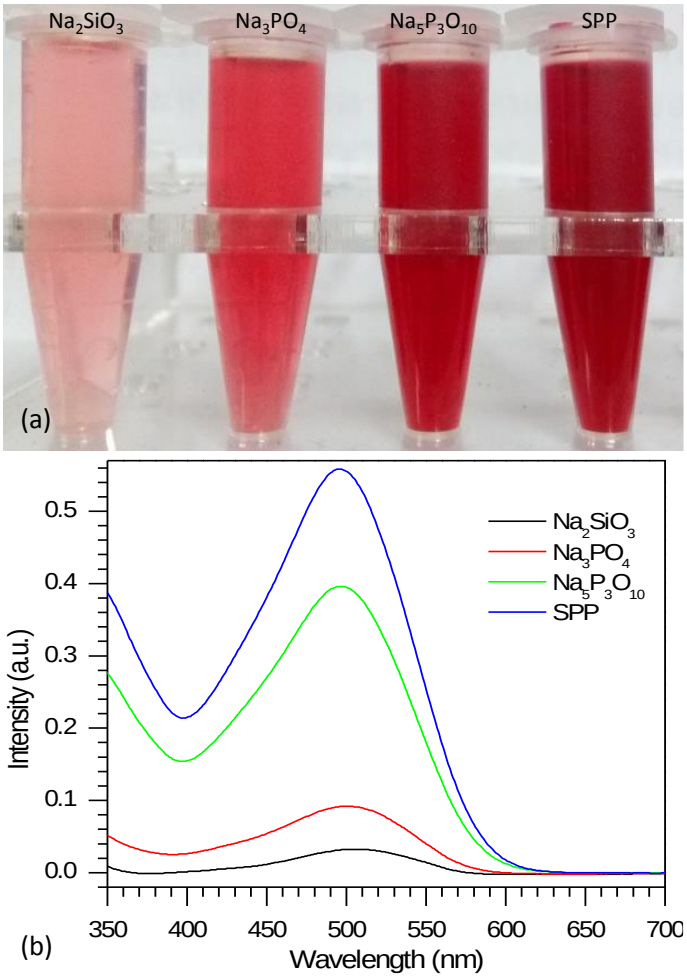

Figure S11. (a) Photograph and (b) UV-vis spectra of initial Congo red solutions (3000 mg L^{-1}) being treated with the MgO particles obtained from the reaction between $Mg(NO_3)_2$ and Na_2CO_3 in the presence of 0.10 g Na_2SiO_3, sodium phosphate (Na_3PO_4), sodium tripolyphosphate ($Na_5P_3O_{10}$) and sodium polyphosphate (SPP).

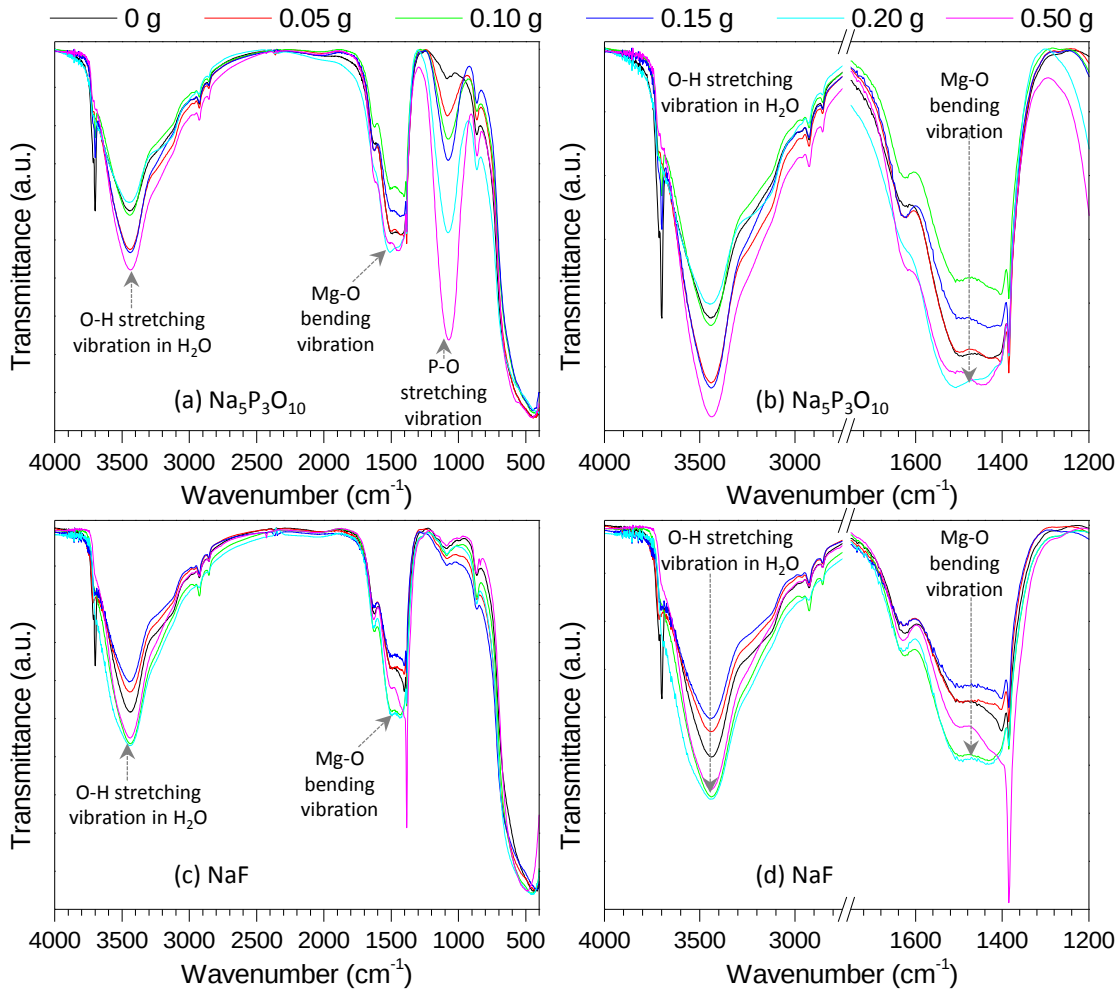

Figure S12. (a) FT-IR spectra of the obtained MgO with varying the added amount of (a-b) $Na_5P_3O_{10}$ and (c-d) NaF in preparation and (b) and (d) their magnified wavenumber range (4000 - 1200 cm^{-1}).

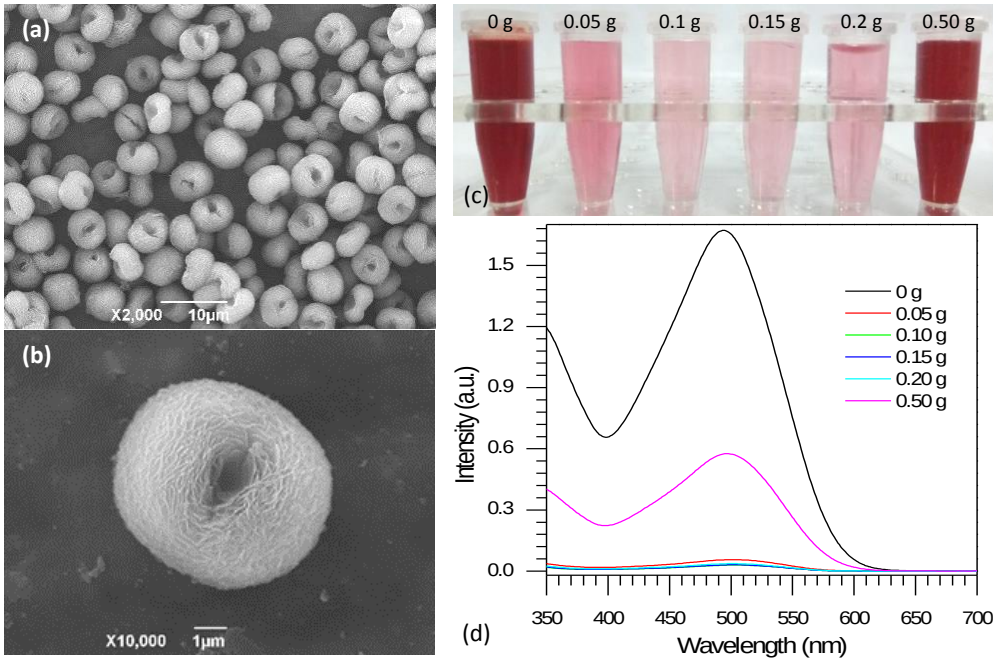

Figure S13. (a-b) Typical SEM images of the obtained MgO particles by reaction of $Mg(NO_3)_2$ and Na_2CO_3 under the temperature of 80 ^oC followed by a period of 1 h aging: (a) panoramic morphology and (b) individual particle; (c) Photograph and (d) UV-vis spectra of initial Congo red solutions (2200 mg L^{-1}) being treated with the MgO particles obtained from the reaction between $Mg(NO_3)_2$ and Na_2CO_3 in the presence of various amounts of Na_2SiO_3 (0 – 0.50 g) as indicated in the figures.

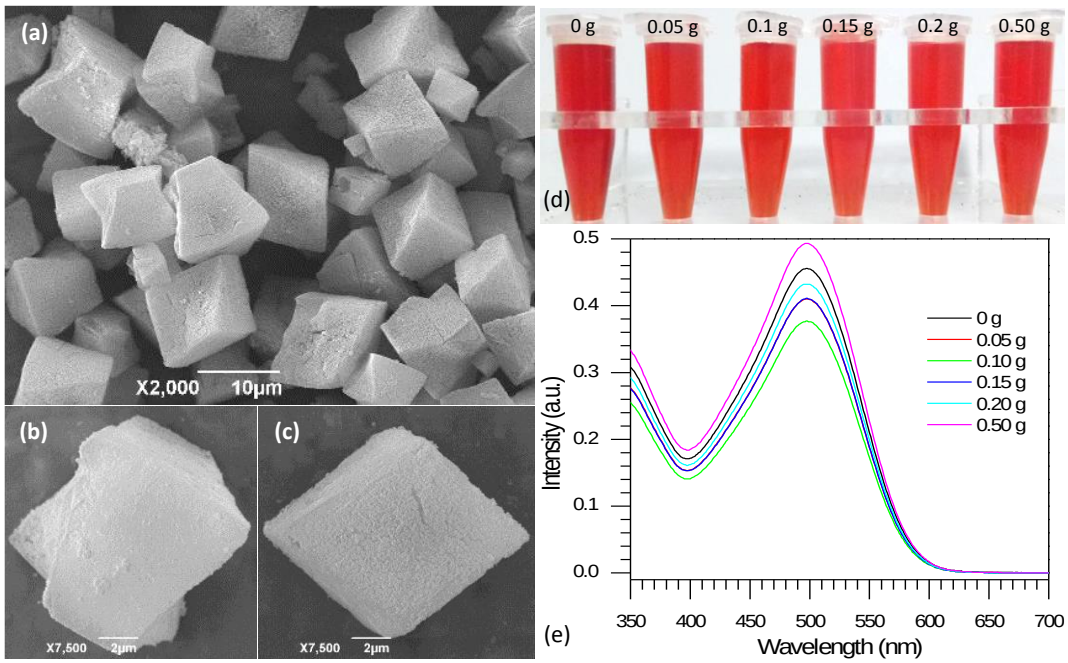

Figure S14. (a-c) Typical SEM images of the obtained MgO particles by reaction of $Mg(NO_3)_2$ and $Na_2C_2O_4$ under the temperature of 50 ^oC: (a) panoramic morphologies; (b) the front view and (c) the side view of a typical particle; (d) Photograph and (e) UV-vis spectra of initial Congo red solutions (500 mg L^{-1}) being treated with the MgO particles obtained from the reaction between $Mg(NO_3)_2$ and $Na_2C_2O_4$ in the presence of various amounts of Na_2SiO_3 (0 – 0.50 g) as indicated in the figures.

Table S1. Adsorption kinetic parameters for the adsorption of Congo red on needle-like MgO without the partition of Na_2SiO_3 in preparation

Initial Concentration (mg L^{-1})	Pseudo-First-Order Model				Pseudo-Second-Order Model			
	Experimental q_e (mg g^{-1})	Calculated q_e (mg g^{-1})	k_1 (g mg^{-1} min^{-1})	R^2	Experimental q_e (mg g^{-1})	Calculated q_e (mg g^{-1})	k_2 (g mg^{-1} min^{-1})	R^2
1000	994.6	73.5	0.115	0.6812	994.6	1000.0	7.7×10^{-3}	1.0000
1500	1493.8	78.0	0.080	0.6291	1493.8	1501.5	2.1×10^{-3}	0.9999
2000	1985.2	752.2	0.077	0.8326	1985.2	2040.8	1.9×10^{-4}	0.9985
2200	2176.7	1148.7	0.068	0.9163	2176.7	2325.6	1.0×10^{-4}	0.9976
2500	2312.5	1525.3	0.070	0.9675	2312.5	2500.0	7.0×10^{-5}	0.9974

Table S2. Adsorption isotherm parameters of Congo red on MgO prepared in the absence and presence of Na_2SiO_3

MgO	Langmuir			Freundlich		
	q_m (mg g^{-1})	b	R^2	K_f	n	R^2
Without Na_2SiO_3	2353	0.2169	0.8991	1166	8.409	0.7279
With Na_2SiO_3	3236	0.1487	0.9705	1448	6.101	0.8931

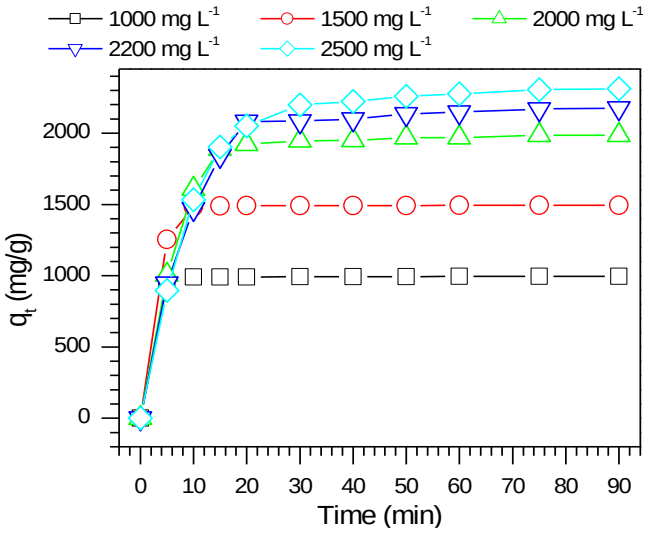

Figure S15. Time profiles of Congo red adsorption at different initial concentrations (1000 – 2500 mg g^{-1}) on as-synthesized MgO from the system without presence of Na_2SiO_3 (MgO concentration: 1.0 g L^{-1})

Table S3. Adsorption capacities of Congo red on various MgO adsorbents

MgO adsorbent	Removal Capacity (mg g^{-1})	Reference
Rod-like MgO	3236	This paper
Lamellar MgO nanostructures	2650	[1]
Porous hierarchical MgO	2409	[2]
Hierarchical MgO nanostructure	1051	[3]
Porous MgO	689	[4]
Porous nanosheet-assembled MgO microrods	480	[5]
Flower-like 3D hierarchical MgO structures	197	[6]
MgO nanoplates	131	[7]
Commercial MgO powders	105	[8]

References

[1] X. Liu, C. Niu, X. Zhen, J. Wang, X. Su, *J. Mater. Res.* **2015**, *30*, 1639-1647.

[2] P. Tian, X.-Y. Han, G.-L. Ning, H.-X. Fang, J.-W. Ye, W.-T. Gong, Y. Lin, *ACS Appl. Mater. Interfaces* **2013**, *5*, 12411-12418.

[3] J. P. Dhal, M. Sethi, B. G. Mishra, G. Hota, *Mater. Lett.* **2015**, *141*, 267-271.

[4] L. Ai, H. Yue, J. Jiang, *Nanoscale* **2012**, *4*, 5401-5408.

[5] T. Wang, Y. Xu, Q. Su, R. Yang, L. Wang, B. Liu, S. Shen, G. Jiang, W. Chen, S. Wang, *Mater. Lett.* **2014**, *116*, 332-336.

[6] S. Li, B. Zhou, B. Ren, L. Xing, L. Tan, L. Dong, J. Li, *Mater. Lett.* **2016**, *171*, 204-207.

[7] J. Hu, Z. Song, L. Chen, H. Yang, J. Li, R. Richards, *J. Chem. Eng. Data* **2010**, *55*, 3742-3748.

[8] X. Li, W. Xiao, G. He, W. Zheng, N. Yu, M. Tan, *Colloids Surf., A* **2012**, *408*, 79-86.